

Measurement of angular dependence of M X-ray production differential cross-sections in heavy elements at 5.96 keV

Rıdvan Durak*

Contribution from: Atatürk University, Faculty of Arts and Science, Department of Physics, Erzurum, Türkiye

Received: August 2, 2005

Accepted (in revised form): January 11, 2006

Abstract

The angular dependence of M X-ray production differential cross-sections for selected heavy elements between Lu and Pt have been measured at 5.59 keV of incident photon energy and at seven emission angles in the range of 120° - 150° using a Si(Li) detector. Angular dependence of M X-ray production differential cross-sections has been derived, using the M-shell fluorescence yields, experimental total M X-ray production cross-sections and theoretical M-shell photoionization cross-sections. M X-ray production differential cross-sections are found to decrease with increase in the emission angle, showing an anisotropic spatial distribution of M X-rays. Extracted results have been compared with the theoretical predictions and semi empirical fits.

Keywords: M X-rays, angular dependence, production differential cross-sections

Résumé

La dépendance angulaire des sections transversales différentielles de production de rayons M X pour des éléments lourds choisis entre Lu et Pt, a été mesurée en utilisant un détecteur de Si(Li), dont l'énergie de photon incident était de 5.59 keV à sept angles d'émission dans la gamme 120° - 150° . Des sections transversales différentielles de production de rayons MX de la dépendance angulaire ont été dérivées en utilisant les rendements de fluorescence de M, les sections transversales expérimentales de production totale de rayons MX et les sections transversales théoriques de photo ionisation de M. On a constaté que les sections transversales différentielles de production de rayons MX diminuent avec l'augmentation de l'angle d'émission.

*Author to whom correspondence should be addressed:
Fax: +90 442 236 09 48; rdur@rocketmail.com (R. Durak)

Cela montre une distribution spatiale anisotrope des rayons M X. Les résultats obtenus ont été comparés aux prévisions théoriques et aux ajustements semi empiriques.

Introduction

The knowledge of the angular dependence of M-shell production differential cross-sections is important because of their extensive use in basic studies of photoelectric effect, characteristic X-ray production, internal conversion of γ -rays, radiative and non-radiative transition probabilities and development of more reliable angular dependence theoretical models describing fundamental inner-shell ionization processes. Experimental and theoretical several attempts have been made for K and L X-ray angular correlation (1-12).

Previous investigators (13-16) have reported that subsequent to photoionization of K and L shell electrons, the emission of the $K\alpha$, $K\beta$, and $L\gamma$ groups of fluorescence X-ray lines is isotropic while that of $L\ell$ and $L\alpha$ groups is anisotropic in spatial distribution. It was concluded that the L_3 vacancy states with $J = 3/2$ are aligned whereas the L_1 and L_2 vacancy states with $J = 1/2$ are non-aligned. According to Cooper and Zare (17), the spatial distribution of X-ray emission for different magnetic substances is always isotropic, but in the theoretical calculations by Papp *et al.* (18), it is shown that the spatial distribution of X-rays is different for different magnetic subshell. Furthermore, the calculations of Cooper and Zare (17) predict that after photoionisation, the inner-shell vacancy state has equal population of magnetic substances and is therefore not alignment. Extensive literature search reveals that the angular dependence of MX-ray production differential cross-sections for the elements Lu, Hf, Ta, W, Os and Pt, especially for the angular range 120° - 150° are not available, due to the complexity associated with the M X-ray spectrum and experimental difficulties.

In view of the above status, we felt necessary to investigate angular dependence of the M X-ray production differential cross-sections. In the present study, we have measured angular dependence of the M X-ray production differential cross-sections for heavy elements Lu, Hf, Ta, W, Os and Pt at 5.96 keV of incident photon energy using a fluorescence excitation technique. The experimental geometry, the method of measurement and experimental results are reported in this paper.

Experimental

The experimental arrangement and geometry used in the present study are shown in Figure 1. The source-target geometry was varied at different angles varying from 120° to 150° at intervals of 5° . The emission angle was set to 0° . The target M X-ray spectra were recorded by the collimated Si(Li) detector, which has an active area of 12.5 mm^2 , a sensitive crystal depth of 3 mm and a Be window of 0.025 mm thickness. The measured energy resolution of the detector system was 188 eV for an amplifier shaping time constant of $6 \mu\text{s}$ at the 5.9 keV peak of ^{55}Fe . The detector was placed in a lead-housing to minimize detection of radiations directly from the source and those scattered from the surroundings. Spectroscopically pure targets of 1.70 cm^2 area and thickness ranging from 3 to 35 mg/cm^2 were used. The spectra were accumulated in time intervals ranging from 43200 s to

280800 s in order to obtain sufficient statistical accuracy and detection limits for low probability events. The M X-rays photo peak areas were evaluated by fitting multi-Gaussian functions plus polynomial background.

Data analysis

Experimental method

The experimental values of angular dependence M X-ray production differential cross-sections for heavy elements were given by:

$$\frac{d\sigma_M^\theta}{d\Omega} = \frac{N_M^\theta}{4\pi(I_0 G)^\theta \varepsilon_M^\theta \beta_M^\theta t} \quad (1)$$

where N_M^θ ($\theta = 120^\circ$ - 150°) are the net counts per unit time under the M X-ray peak, $(I_0 G)^\theta$ is the intensity of exciting radiation falling on the portion of sample visible to the detector, ε_M^θ is the detector efficiency for the M X-rays of the element, t is the mass per unit area of the element (g cm^{-2}) and β_M^θ is the absorption-correction factor that accounts for absorption of the incident photons and emitted M X-rays in the target is the self absorption correction factor of the target material and is given by:

$$\beta_M^\theta = \frac{1 - \exp[-(\mu_i \sec \phi + \mu_e \sec \alpha)t]}{(\mu_i \sec \phi + \mu_e \sec \alpha)t} \quad (2)$$

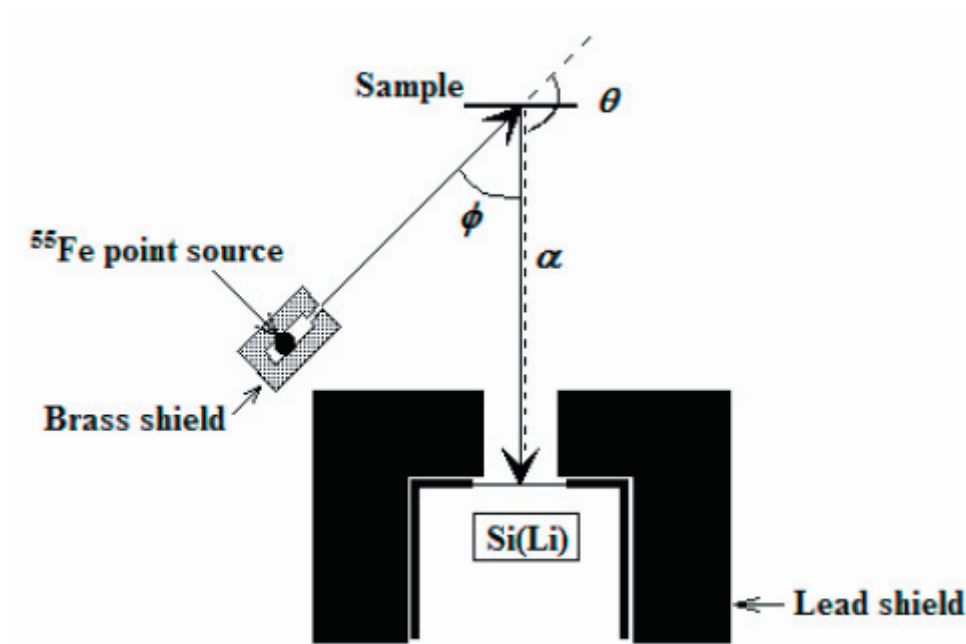


Figure 1. Experimental set-up used for measurements of angular dependence M X-ray production cross-section.

where μ_i and μ_e are the total mass absorption coefficients of target material at the incident photon and emitted *M* X-rays energies, respectively (19). *t* is the thickness of the sample. ϕ and α are the angles of the incident and emitted X-ray with respect to the target normal, ϕ and α were set to 30°-60° and 0°, respectively, in the present set-up. In this study, the values of $(I_0 G \varepsilon_M)^\theta$ were determined by collecting the *K* X-ray yields from thin standard samples of Al, Si, P, S, Cl, K, Ca and Ti using the relation:

$$(I_0 G \varepsilon_K)^\theta = \frac{N_K^\theta}{\sigma_K^x(E) \beta_K^\theta t} \quad (3)$$

where N_K^θ , β_K^θ and ε_K are defined as in Equation 1. However, for *K* instead of *M* X-rays. σ_K^x values were derived:

$$\sigma_K^x = \sigma_K^p(E) \omega_K \quad (4)$$

where $\sigma_K^p(E)$ is the *K* shell photoionization cross-section for the element at excitation energy *E* from tables of Scofield (20) and ω_K is *K* shell fluorescence yields from tables of Hubbell (21). The measured $(I_0 G \varepsilon_K)^\theta$ ($\theta = 120^\circ$) values for the present set-up are plotted as a function of

energy in Figure 2.

Theoretical model

The theoretical *M* X-ray production differential cross-sections values for heavy elements were deduced from the relation:

$$\frac{d\sigma_M}{d\Omega} = \frac{\sigma_M^p(E) \omega_M}{4\pi} \quad (5)$$

where $\sigma_M^p(E)$ is the *M* shell photoionization cross-section for the element at excitation energy *E* from tables of Scofield (20) and ω_M is the *M* shell fluorescence yields from tables of Hubbell (21).

Results and Discussion

The present measured *M* X-rays production differential cross-sections in Lu, Hf, Ta, W, Os and Pt at 5.96 keV of incident photon energy in the angular range 120°-150° are listed in Table 1 and they are compared with the available theoretical predictions and fitted values. The experimental results are represented graphically as *M* X-rays production differential cross-sections vs. $\cos\theta$ ($\theta = 120^\circ$ -150°) in Figures 3(a)-(f). It has been observed that *M* X-ray production differential cross-sections decrease with increase in the emission angle. Present experimen-

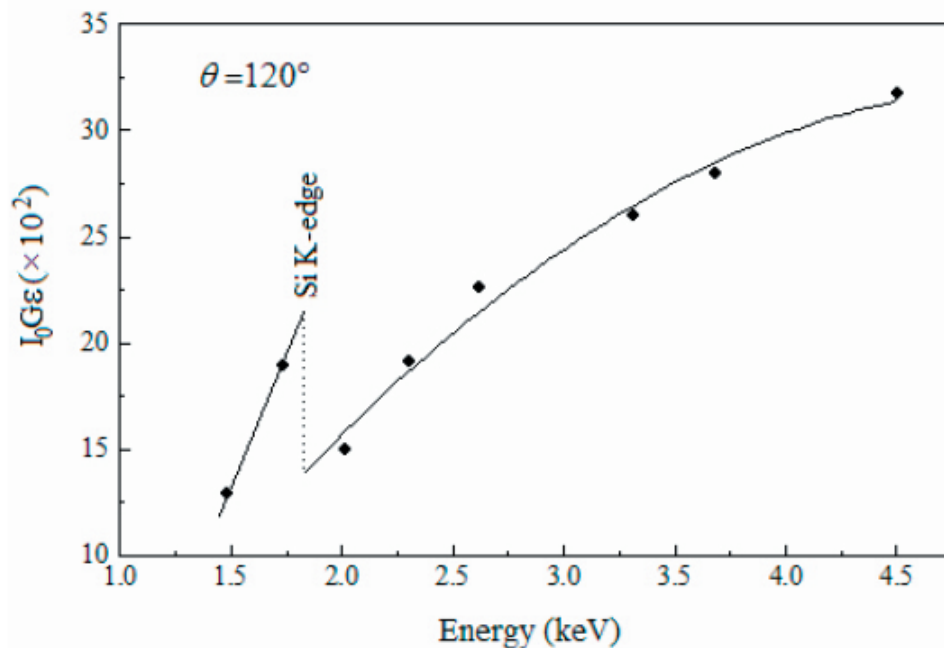


Figure 2. Plot of the factor vs. *K* X-ray energy.

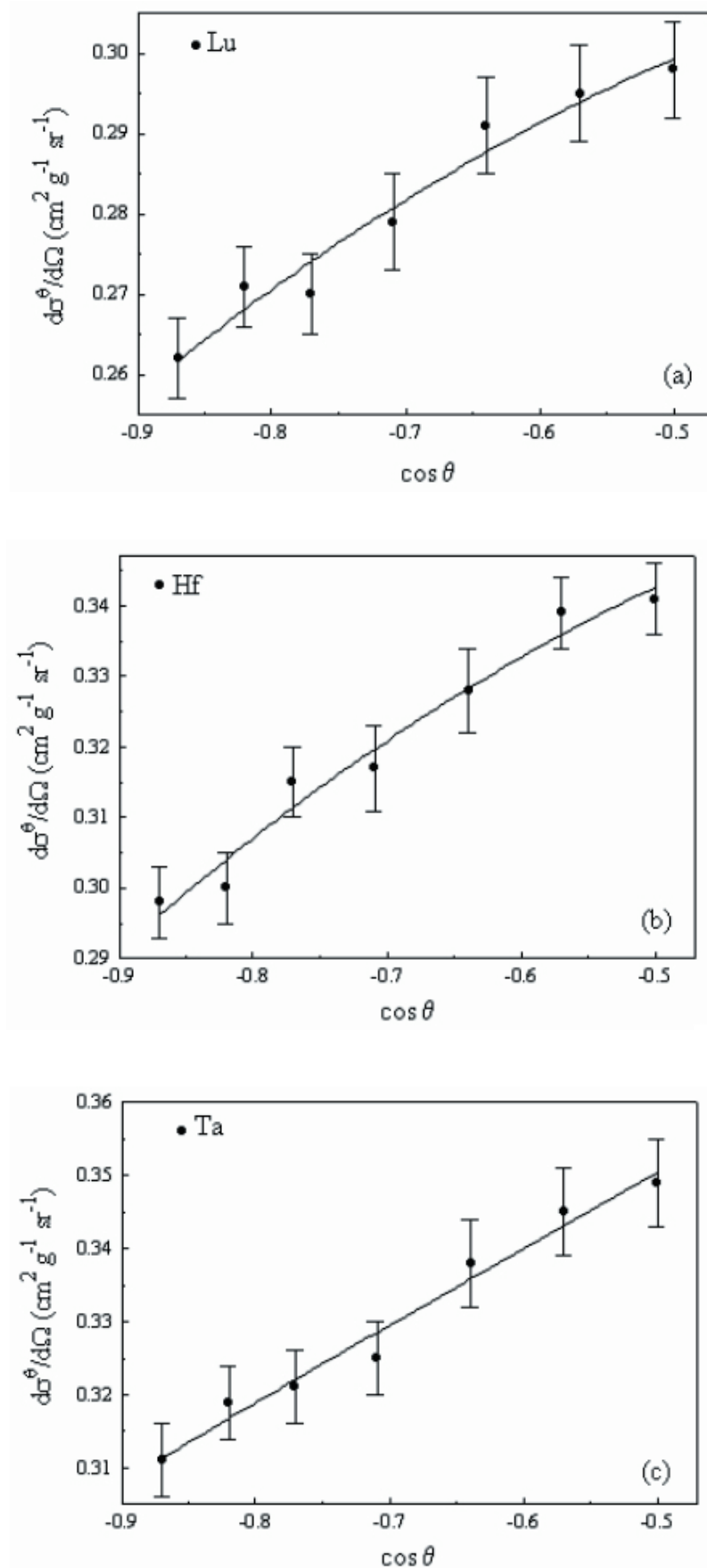


Figure 3. The measured values of the angular dependence MX -rays production differential cross-sections are plotted as a function of $\cos \theta$ for a) Lu, b) Hf c) Ta.

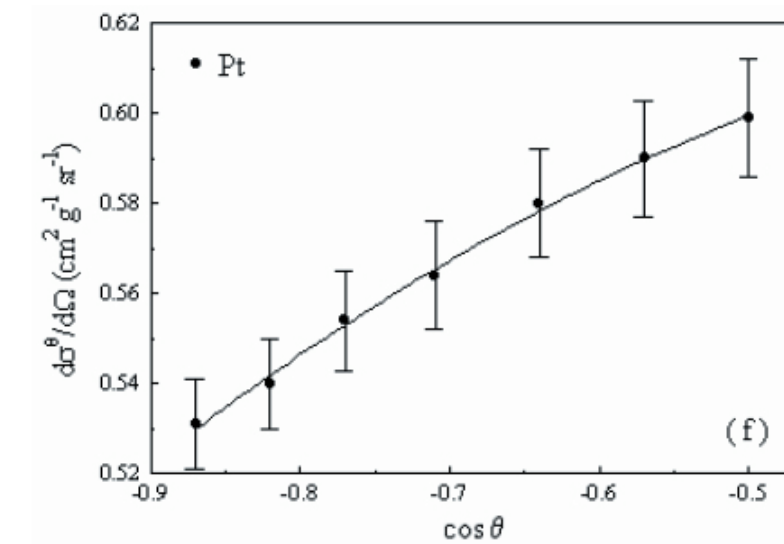
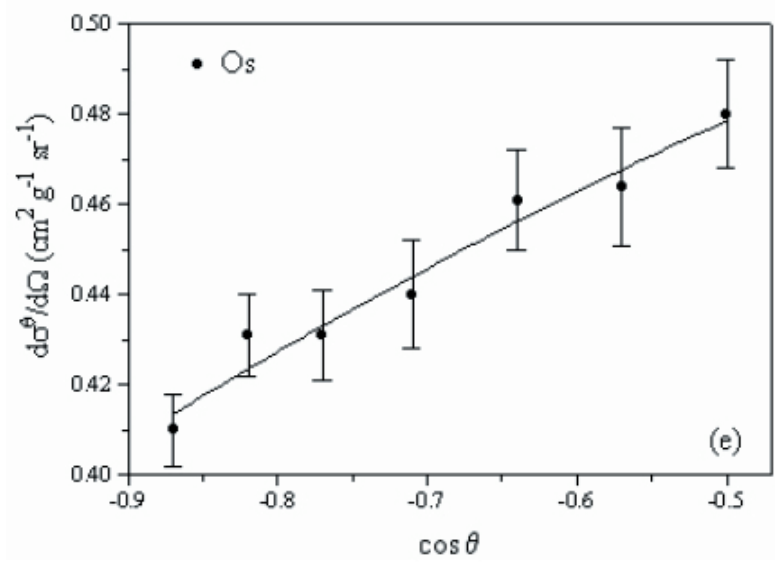
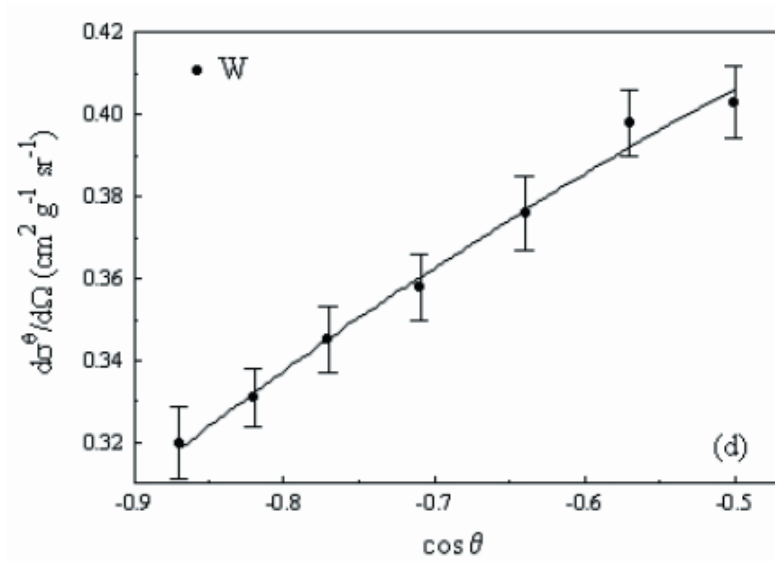


Figure 3 continued. The measured values of the angular dependence M X-rays production differential cross-sections are plotted as a function of $\cos \theta$ for d) for W, e) for Os, f) Pt.

Table 1. Comparison of present experimental, theoretical and fitted M X-ray production differential cross-sections ($cm^2/g sr$).

Lu			Hf			Ta			
$\theta(^{\circ})$	Experimental	Fitted	Theo.	Experimental	Fitted	Theo.	Experimental	Fitted	Theo.
120	0.298 ± 0.006	0.299		0.341 ± 0.005	0.337		0.349 ± 0.006	0.350	
125	0.295 ± 0.006	0.294		0.339 ± 0.005	0.329		0.345 ± 0.006	0.343	
130	0.291 ± 0.006	0.288		0.328 ± 0.006	0.321		0.338 ± 0.006	0.335	
135	0.279 ± 0.006	0.281	0.293	0.315 ± 0.005	0.312	0.325	0.325 ± 0.005	0.338	0.362
140	0.270 ± 0.005	0.274		0.317 ± 0.005	0.303		0.321 ± 0.005	0.322	
145	0.271 ± 0.005	0.268		0.300 ± 0.005	0.295		0.319 ± 0.005	0.317	
150	0.262 ± 0.005	0.262		0.298 ± 0.005	0.286		0.311 ± 0.005	0.311	
W			Os			Pt			
$\theta(^{\circ})$	Experimental	Fitted	Theo.	Experimental	Fitted	Theo.	Experimental	Fitted	Theo.
120	0.403 ± 0.009	0.406		0.480 ± 0.012	0.479		0.599 ± 0.013	0.600	
125	0.398 ± 0.008	0.392		0.464 ± 0.013	0.468		0.590 ± 0.013	0.589	
130	0.376 ± 0.009	0.377		0.461 ± 0.011	0.456		0.580 ± 0.012	0.578	
135	0.358 ± 0.008	0.360	0.401	0.440 ± 0.012	0.444	0.487	0.564 ± 0.012	0.565	0.595
140	0.345 ± 0.008	0.345		0.431 ± 0.010	0.433		0.554 ± 0.012	0.553	
145	0.331 ± 0.007	0.332		0.431 ± 0.009	0.423		0.540 ± 0.010	0.542	
150	0.320 ± 0.009	0.318		0.410 ± 0.008	0.413		0.531 ± 0.010	0.530	

Table 2. Angular dependence M X-ray production cross-sections fitted to the $\sum_n A_n Z^n$ as a function of $\cos \theta$ ($\theta = 120^{\circ} - 150^{\circ}$).

Elements	Fitting coefficient		
	A_0	A_1	A_2
Lu	0.31498	-0.00911	-0.08070
Hf	0.36150	-0.01271	-0.10098
Ta	0.40039	0.09689	-0.00623
W	0.47394	0.07704	-0.11696
Os	0.53632	0.08100	-0.06891
Pt	0.62229	-0.03649	-0.16409

Table 3. Uncertainties in the quantities used to determine angular dependence M X-ray production differential cross-sections in Equation 1.

Quantity	Nature of uncertainty	Uncertainty (%)
N_M^{θ}	Counting statistics	2
$(I_0 G \epsilon)^{\theta}$	Errors in different parameters used to evaluate this factor	4
β_M^{θ}	Error in the absorption coefficients at incident and emitted photon energies	< 1
t	Nonuniform thickness	1

tal values were fitted to a second-order polynomial as a function of $\cos\theta$ and fitted values in the same table. The fitted coefficients are listed in Table 2. Using our fitted values, the experimental angular dependence *MX*-rays production differential cross-sections for all elements in the range $71 \leq Z \leq 78$ can be obtained for comparison and the fit will be valid in the seven angles from 120° to 150° .

The overall error in the measured angular dependence *MX*-ray production differential cross-sections are estimated to be less than 1.5 % - 2.8 %, which arises due to the uncertainties in the various physical parameters required to evaluate the experimental results using Equation 1. The uncertainties in the parameters are listed in Table 3. It is evident from Table 1 and Figure 3 that the present experimental results are in good agreement with the theoretical values.

Conclusion

The angular dependence *MX*-ray production differential cross-sections are found to decrease with increase in the emission angle, showing anisotropic spatial distribution. To the best of our knowledge, no other experimental results are available for worked elements in the angular range 120° - 150° for comparison with present results. Therefore, the results obtained in the present study constitute the first experimental measurements.

Consequently, much more experimental information will need to be available before a meaningful comparison of experiment and theory becomes possible.

Acknowledgments

The author would like to thank Dr. Yüksel Özdemir for contributions to the manuscript. The author also wishes to thank Dr. Abdullah Er for translating the English abstract into French.

References

1. R. Anholt, J.O. Rasmussen, *Phys. Rev. A*, **9**, 585 (1974).
2. A.L. Catz, *Phys. Rev. A*, **3**, 849 (1970).
3. A.L. Catz, E.S. Macias, *Phys. Rev. A*, **3**, 849 (1971).
4. M. Ertuğrul, E. Büyükkasap, A. Küçükönder, A.İ. Kopya, H. Erdoğan, *Nuova Cimento*, **17**, 993 (1995).
5. M.R. Zalutsty, E.S. Macias, *Phys. Lett. A*, **49**, 285 (1974).
6. J.H. Scofield, *Phys. Rev. A*, **40**, 3054 (1989).
7. J.H. Scofield, *Phys. Rev. A*, **14**, 1418 (1976).
8. J.W. Cooper, R.N. Zare, *J. Chem. Phys.*, **48**, 942 (1968).
9. K. Bulum, H. Kleinpopen, *Phys. Rep.*, **52**, 203 (1979).
10. K. Bulum, H. Kleinpopen, *Phys. Rep.*, **96**, 251 (1983).
11. J.W. Cooper, R.N. Zare, *J. Chem. Phys.*, **48**, 942 (1968).
12. M. Ertuğrul, R. Durak, E. Tıraşoğlu, E. Büyükkasap, H. Erdoğan, *Appl. Spectrosc. Rev.*, **30**, 219 (1995).
13. K.S. Kahlon, K. Shatentra, K.L. Allawadhi, B.S. Sood, *Pramana-J. Phys.*, **35**, 105 (1990).
14. K.S. Kahlon, H. Aulakh, S. Singh, N.R. Mittal, K.L. Allawadhi, B.S. Sood, *Phys. Rev. A*, **43**, 1455 (1991).
15. K.S. Kahlon, H. Aulakh, S. Singh, N.R. Mittal, K.L. Allawadhi, B.S. Sood, *Phys. Rev. A*, **44**, 4379 (1991).
16. K.S. Kahlon, K.L. Allawadhi, B.S. Sood, *J. Phys. B: At. Mol. Opt. Phys.*, **32**, 3701 (1991).
17. J.W. Cooper, R.N. Zare, "Atomic Collisions Processes", Vol. XIC. Gordon and Breach, New York 1969, p.317.
18. T. Papp, J. Polinkas, L. Sarkadi, *Phys. Rev. A*, **42**, 5452 (1990).
19. J.H. Hubbell, S.M. Seltzer, National Institute of Standards and Technology Report No. NISTIR 5632, (1995).
20. J.H. Scofield, Lawrence Livermore National Report No. UCRL 51326, (1973).
21. J.H. Hubbell, P.N. Trehan, N. Singh, B. Chand, D. Mehta, M.L. Garg, R.R. Garg, S. Singh, S. Puri, *J. Phys. Chem. Ref. Data*, **23**, 339 (1994).